Journal of Hazardous Materials 177 (2010) 711–718

Contents lists available at ScienceDirect

Journal of Hazardous Materials

journal homepage: www.elsevier.com/locate/jhazmat

Comparative study of the cytotoxic and genotoxic effects of titanium oxide and aluminium oxide nanoparticles in Chinese hamster ovary (CHO-K1) cells

A.L. Di Virgilio[a], M. Reigosa[b], P.M. Arnal[a,1], M. Fernández Lorenzo de Mele[a,*]

[a] Instituto de Investigaciones Fisicoquímicas Teóricas y Aplicadas (INIFTA), Diag. 113 y 64, Correo 16, Suc. 4, La Plata (1900), Argentina
[b] Instituto Multidisciplinario de Biología Celular (IMBICE), Calle 526 y Camino Gral. Belgrano (entre 10 y 11), La Plata (1900), Argentina

ARTICLE INFO

Article history:
Received 13 August 2009
Received in revised form
18 December 2009
Accepted 18 December 2009
Available online 29 December 2009

Keywords:
Titanium oxide
Aluminium oxide
Nanoparticles
Cytotoxicity
Genotoxicity
Cell culture

ABSTRACT

The aim of this study was to analyze the cytotoxicity and genotoxicity of titanium oxide (TiO_2) and aluminium oxide (Al_2O_3) nanoparticles (NPs) on Chinese hamster ovary (CHO-K1) cells using neutral red (NR), mitochondrial activity (by MTT assay), sister chromatid exchange (SCE), micronucleus (MN) formation, and cell cycle kinetics techniques. Results showed a dose-related cytotoxic effect evidenced after 24 h by changes in lysosomal and mitochondrial dehydrogenase activity. Interestingly, transmission electronic microscopy (TEM) showed the formation of perinuclear vesicles in CHO-K1 cells after treatment with both NPs during 24 h but no NP was detected in the nuclei. Genotoxic effects were shown by MN frequencies which significantly increased at 0.5 and 1 μg/mL TiO_2 and 0.5–10 μg/mL Al_2O_3. SCE frequencies were higher for cells treated with 1–5 μg/mL TiO_2. The absence of metaphases evidenced cytotoxicity for higher concentrations of TiO_2. No SCE induction was achieved after treatment with 1–25 μg/mL Al_2O_3. In conclusion, findings showed cytotoxic and genotoxic effects of TiO_2 and Al_2O_3 NPs on CHO-K1 cells. Possible causes of controversial reports are discussed further on.

© 2010 Elsevier B.V. All rights reserved.

1. Introduction

Nanomaterials are designed structures of at least one dimension of 100 nm or less. These materials are present in a number of commercially available products including fillers, catalysts, cosmetics, and many industrial applications. TiO_2 NPs are used for protection against UV ray exposure due to their high refractive index. Many sunscreens contain these NPs as well as surface coating products which are colorless and reflect and scatter UV rays more efficiently than larger particles [1–3]. Nanosized Al-containing particles are also used in industrial, domestic, and medical products, energetic systems (composite propellants), to replace lead primers in artillery, etc.

There is scarce information about the possible toxic effects of NPs on health and environment despite of their current use in novel technology. Since the risks of exposure to nanomaterials are still unknown, alarming speculations are put forward [4].

NP properties differ substantially from bulk material with similar composition, allowing them to exhibit unusual values of reactivity, conductivity, and optical sensitivity among other properties. These capabilities may yield harmful interactions with biological systems and the environment, with potentially toxic effects [5–9]. Thus, the evaluation of their toxicity is essential.

On the other hand, the toxic action of most biomaterial components in consumer goods has been so far evaluated at macroscale with well established toxicity assessment methods. However, those methods have not been frequently employed for materials at nanoscale dimension [8]. There are some few studies on the toxicological effects of *in vitro* exposure to this type of manufactured nanomaterials. In fact, the development of new toxicity assessment methods for NPs has been suggested [9].

The toxicity of several metal oxide NPs such as TiO_2, ZnO, and Fe_2O_3 has been analyzed using different cell lines. A complete review about this issue has been recently reported [10]. Few studies on the toxicity of Al-containing particles have so far been published. Some articles report micronuclei increase [11], DNA damage detected by Comet assay [12] and chromosomal aberrations [13] caused by $AlCl_3$ NPs. In the case of Al_2O_3 NPs, reports are even more limited. Rat bone marrow [14] and alveolar macrophages (NR8383) [15] were used. Lower toxicity of Al_2O_3 NPs than Al NPs was found.

CHO-K1 cells have also been used as a mammalian cell line model in several research studies. However there are controversial reports. Theogaraj et al. [16] and Warheit et al. [17] did not find TiO_2 NPs to be genotoxic since they did not observe DNA damage frequency increase after the chromosomal aberration test in CHO cells. Conversely, Nakagawa et al. [18], Lu et al. [19], Uchino et al. [20], and Zhu et al. [21] found toxic effects of TiO_2 on this cell line. However, in some cases NPs used were not characterized.

* Corresponding author. Tel.: +54 221 4257291; fax: +54 221 4254642.
E-mail address: mmele@inifta.unlp.edu.ar (M. Fernández Lorenzo de Mele).
[1] Formerly at: Max Planck Institut für Kohlenforschung, Kaiser-Wilhelm-Platz 1, 45470 Mülheim an der Ruhr, Germany.

0304-3894/$ – see front matter © 2010 Elsevier B.V. All rights reserved.
doi:10.1016/j.jhazmat.2009.12.089

In an attempt to elucidate the causes of the apparently inconsistent results found for TiO_2 NPs and to complement scarce previous information on Al_2O_3 NPs, several end points rigorously and carefully performed with previously characterized TiO_2 and Al_2O_3 NPs were assayed in CHO-K1 cell line in order to analyze both cyto- and genotoxic effects. Following this purpose, cytotoxicity was determined and NPs concentration range free of cytotoxic effects was identified in CHO-K1 cells. Afterwards, the analysis of genotoxicity at this low concentration level (from 1 μg/mL up to the previously identified threshold value) was performed.

2. Materials and methods

2.1. Chemicals

Titanium oxide NPs were purchased from Aldrich (Milwaukee, WI, USA) and aluminium oxide NPs from Sigma–Aldrich (St. Louis, MO, USA). We estimated mean particle diameters and the corresponding errors using transmission electron microscopic (TEM) images from commercially available nanoparticles.

Nanoparticle stock suspensions were prepared in phosphate buffered saline (PBS), vortexed for 10 min and stored at 4 °C in the dark. All other chemicals were of highest quality available.

2.2. Characterization of TiO_2 and Al_2O_3 NPs

Shape, size distribution, and specific surface area of TiO_2 and Al_2O_3 NPs were characterized. The first two determinations were measured with transmission electronic microscopy (TEM) and the third one with nitrogen sorption. TEM-pictures were obtained with a Hitachi H-7500 microscope operated at 100 kV. Solid samples were dried on the sample holder (Lacey-Carbon, 400 mesh, 3.05 mm) and analyzed without further treatment under ultra high vacuum. For nitrogen sorption measurements a Micromeriticas ASAP 2010 adsorption unit was used. Prior to measurement, oxides were activated under vacuum at 423 K for at least 2 h. Measurements were performed at 77 K using a static–volumetric method. The empty volume was determined by He.

2.3. Cell culture

Chinese hamster ovary cells (CHO-K1 line) were originally obtained from the American Type Culture Collection (ATCC, CRL 1661, Rockville, MD, USA). CHO-K1 cells were grown as monolayers in Falcon T-25 flasks with Ham F10 culture medium (GIBCO-BRL, Los Angeles, USA) supplemented with 10% inactivated fetal calf serum (Natocor, Carlos Paz, Córdoba, Argentina), 50 IU/mL penicillin and 50 μg/mL streptomycin sulfate (complete culture medium) in a humidified incubator at 37 °C and 5% CO_2 atmosphere. When 70–80% confluence was reached, cells were subcultured using 0.25% trypsin–1 mM EDTA (ethylenediaminetetraacetic acid) in Ca^{2+}–Mg^{2+} free PBS. Cells were counted in a Neubauer haemocytometer by the exclusion Trypan Blue (Sigma, St. Louis, MO, USA) method.

2.4. Cytotoxicity assays

Two methods were used for determining TiO_2 and Al_2O_3 NPs cytotoxicity in cell cultures since trials with more than one assay are recommended in order to determine cell viability [22]. These methods were the NR uptake assay and the determination of mitochondrial activity with the MTT test. The NR assay is used to measure the population growth of cultured cells; the NR dye is taken up by viable cells and transports it to the lysosome. These processes require energy as well as intact cellular and lysosomal structures. The MTT assay is based on the conversion of the tetrazolium salt by mitochondrial succinic dehydrogenases as marker of cell viability [23]. The tetrazolium ring is cleaved in active mitochondria, and so the reaction takes place only in living cells.

2.4.1. Neutral red uptake assay

The neutral red accumulation assay was performed according to Borenfreund and Puerner [24]. A total of 2.5×10^4 cells/well was plated in 96-well tissue-culture plates. Cells were treated with different NP concentrations for 24 h at 37 °C in 5% CO_2 in air. After treatment, the medium was replaced by a new one containing 100 μg/mL neutral red (NR) dye (Sigma, St. Louis, MO, USA), and cells were incubated for 3 h. Then, neutral red medium was discarded, cells were rinsed twice with warm (37 °C) PBS (pH 7.4) in order to remove the non-incorporated dye, and 100 μl of 50% ethanol, 1% acetic acid solution was added to each well to fix the cells releasing the neutral red into solution. The plates were shaken for 10 min, and solution absorbance in each well was measured in a Microplate Reader (7530, Cambridge Technology, Inc., USA) at 540 nm, and compared with wells containing untreated cells. Absorbance values were corrected by a blank of NPs (cells treated with different NP concentrations, not dye-treated). Cell viability was plotted as percent of control (assuming data obtained in the absence of NPs as 100%).

2.4.2. MTT (methyl tetrazolium) assay

The MTT assay was carried out following a report previously published [25]. Briefly, 2.5×10^4 cells/well were seeded in a 96-multiwell dish, allowed to attach for 24 h, and treated with different NP concentrations for 24 h. After this treatment, the medium was changed and cells were incubated with 0.5 mg/mL MTT (Sigma–Aldrich, St. Louis, MO, USA) under normal culture conditions for 3 h. Cell viability was marked by the conversion of the tetrazolium salt MTT (3-(4,5-dimethylthiazol-2-yl)-2,5-diphenyltetrazolium-bromide) to a colored formazan by mitochondrial dehydrogenases. Color development was measured photometrically in a Microplate Reader (7530, Cambridge Technology, Inc., USA) at 570 nm after cell lyses in DMSO (100 μl/well). Absorbance values were also corrected by a blank of NPs. Cell viability is shown graphically as percent of the control values (cells grown in medium without NPs).

2.5. Sister chromatid exchange (SCE) test and cell cycle kinetics

CHO-K1 cells were cultured with different NP concentrations in the presence of the 10 μg/mL 5′-bromo-2′deoxyuridine (BrdUrd) (Sigma, St. Louis, MO, USA) and incubated under complete darkness for 24 h. Two hours before fixation, cells were treated with colchicine (Sigma, St. Louis, MO, USA) (1 μg/mL final concentration). Air-dried slides were prepared following routine protocols, and differential staining of sister chromatides was obtained according to Wolff and Perry [26]. Each treatment was repeated twice and a total of 100 metaphases were scored per treatment (50 per repetition). Data were expressed as the mean number of SCEs per cell ± SEM.

On the other hand, a minimum of 100 metaphase cells per treatment were scored to determine the percentage of cells which had undergone one (M_1), two (M_2), and three or more mitoses (M_{3+}).

The proliferative rate index (PRI) was calculated for each experimental point according to the following formula: $PRI = [(\%M_1) + 2(\%M_2) + 3(\%M_{3+})]/100$, which indicated the average number of times cells divided in the medium after the addition of BrdUrd until harvesting [27].

2.6. Cytokinesis-block micronucleus (CBMN)

Cytokinesis-block micronucleus technique was performed according to Fenech [28]. Briefly, cells were seeded on coverslips and incubated at 37 °C for 24 h. Then the medium was changed, and the NPs were added along with cytochalasin B (4.5 μg/mL). After 24 h, cells were rinsed and subjected to hypotonic conditions with 0.075% KCl at 37 °C for 5 min, fixed with pure methanol at −20 °C for 10 min. Cells were air-dried, stained with 5% Giemsa solution and mounted on slides for microscopic observation. The assay was carried out three independent times and 1000 binucleated cells per slide were scored.

2.7. Uptake of NPs by CHO-K1 cells and their subcellular localization by TEM

CHO-K1 cells were plated in 24-well plates (4×10^4 cells/mL) and incubated at 37 °C for 24 h. After this incubation period, cells were treated with TiO_2 or Al_2O_3 NPs (50 μg/mL) for 24 h. After incubation, monolayers were rapidly washed three times with serum free medium and fixed with 2% glutaraldehyde in 0.1 M sodium cacodylate buffer for 1 h at 4 °C. After post-fixation in 2% OsO4 in 0.1 M sodium cacodylate buffer for 1 h at 4 °C, samples were embedded in epoxy resin, Epon (Serva, Heidelberg, Germany) and ultra thin sections (60 nm) were obtained by ultramicrotom (Supernova Reichert-J). These sections were stained with 8% uranyl acetate solution in 0.5% acetic acid, and plumbic citrate. Morphologic characteristics of the cells and the distribution of particles within the cells were analyzed placing the ultra thin sections on 150 mesh grids and were then examined by TEM (JEOL JEM 1200 EX II).

2.8. Statistical analysis

At least three independent experiments were performed by triplicate for each experimental condition. Data are expressed as mean ± SEM. The two-tailed Student's *t*-test was used to compare pooled data from independent experiments as mean values for SCE/cell, MTT, and neutral red data between treated and control groups. χ^2 test allowed to obtain cell cycle progression and MN data.

3. Results

3.1. NPs characterization

Shape, diameter distribution, and specific surface area of TiO_2 and Al_2O_3 NPs were experimentally obtained. TiO_2 NPs shape is complex while that of Al_2O_3 is spherical. Hence, an estimation of the particle size distribution for the latter case was straightforward (*i.e.* measurement of diameters) while for TiO_2 different options were available. Among them, we chose the largest length as characteristic dimension. Thus, average particle sizes for TiO_2 and Al_2O_3 were 20 ± 7 nm and 28 ± 19 nm, calculated from 146 and 153 measurements, respectively (±σ error). NPs specific surface area was calculated by the Brunauer–Emmett–Teller (BET) method from the nitrogen sorption isotherm (TiO_2 = 142 $m^2\ g^{-1}$/Al_2O_3 = 39 $m^2\ g^{-1}$).

3.2. Cytotoxic assay analysis and cell viability

TiO_2 and Al_2O_3 NPs cytotoxicity was assayed in 24 h-exposed CHO-K1 cells. Figs. 1 and 2 show the relationship between cell viability (as percentage absorbance of control value) and NPs concentration. NR uptake assay showed a significant decrease in the absorbance up to 25 and 100 μg/mL for TiO_2 and Al_2O_3 respectively (Fig. 1). The strongest effect was observed for TiO_2 which showed 40% absorbance decrease for 100 μg/mL compared with

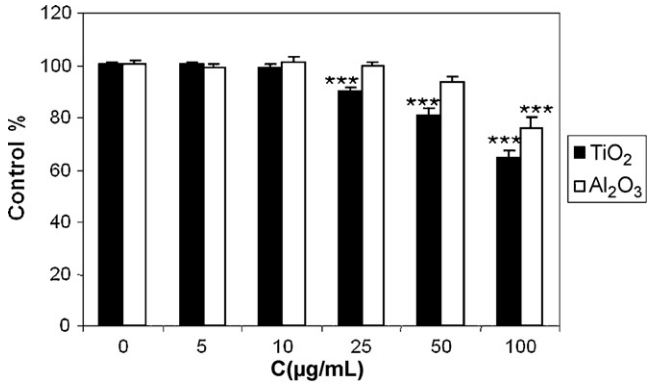

Fig. 1. Neutral red uptake assay in CHO-K1 cells after 24 h exposure to TiO_2 and Al_2O_3 nanoparticles. Significant difference at $^{***}p < 0.001$.

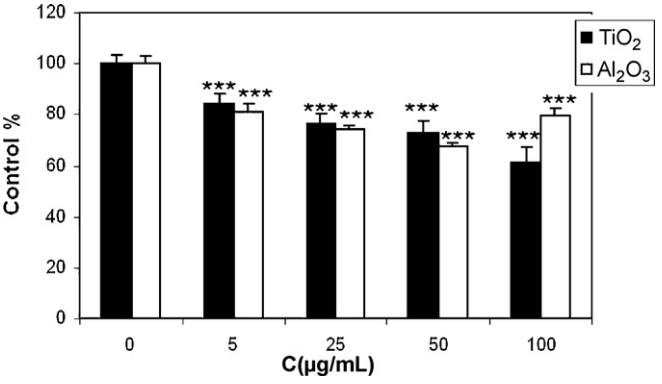

Fig. 2. MTT assay in CHO-K1 cells after 24 h exposure to TiO_2 and Al_2O_3 nanoparticles. Significant difference at $^{***}p < 0.001$.

the control group. A lower decrease was shown by Al_2O_3 for the same concentration.

Results from MTT assays are depicted in Fig. 2. In presence of TiO_2 and Al_2O_3 NPs, a significant absorbance decrease was observed for concentration values equal to or higher than 5 μg/mL.

3.3. Sister chromatid exchange (SCE) and cell cycle kinetics analyses

Fig. 3 shows the results from SCE analysis in CHO-K1 cells treated with different NP concentrations during two cellular cycles. SCE frequencies observed for 1 and 5 μg/mL TiO_2 were significantly higher than those of control cultures ($p < 0.01$). At higher TiO_2 NP concen-

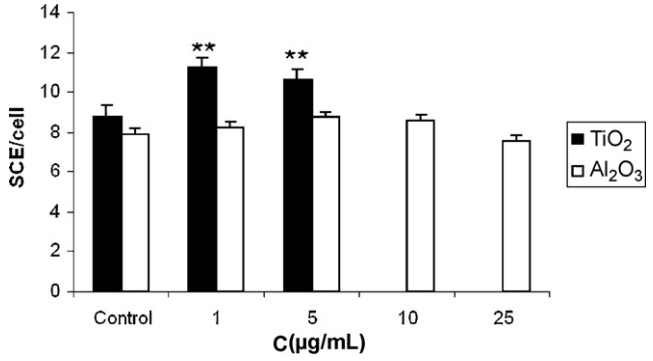

Fig. 3. Sister chromatid exchange (SCE) frequencies in CHO-K1 cells treated with TiO_2 and Al_2O_3 nanoparticles. Significant difference at $^{**}p < 0.01$. Data from TiO_2 NPs highest concentration (10 and 25 μg/mL) could not be measured due to cytotoxic effects.

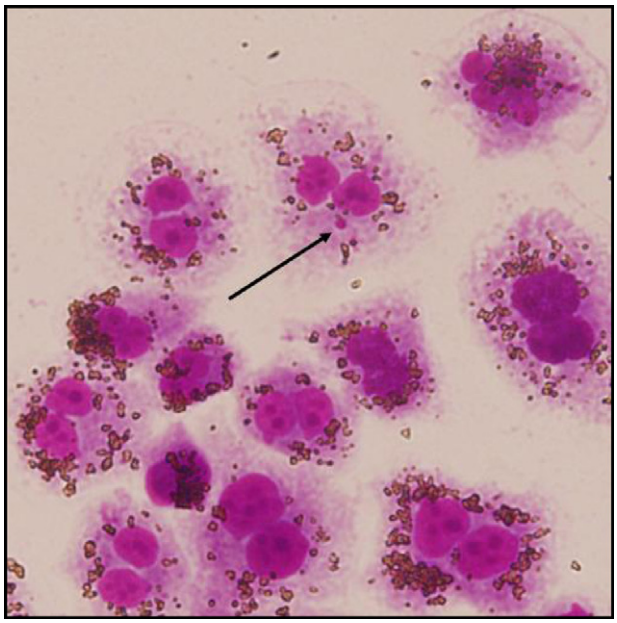

Fig. 4. CHO-K1 cells exposed to TiO_2 (5 g/mL) showing micronucleus induction (see the arrow).

trations, the absence of metaphases indicated overt cytotoxicity. On the other hand, cells treated with Al_2O_3 NPs did not show any increase in SCE frequency.

Cell cycle kinetics was also studied. Results reveal PRI reduction (although not statistically significant) compared with control values at concentrations higher than 10 μg/mL TiO_2 and 25 μg/mL Al_2O_3 NPs.

3.4. Micronucleus frequency

MN formation in binucleated cells were observed after treatment with different concentrations of either TiO_2 or Al_2O_3 NPs (0.5, 1, 5, 10 μg/mL) for 24 h. Fig. 4 shows MN formation in CHO-K1 binucleated cells treated with 5 μg/mL TiO_2.

Al_2O_3 NPs induced a dose-dependent response of MN frequency in the whole range studied, while TiO_2 NPs produced a slight increase at 0.5 and 1 μg/mL but no further increase in MN frequency (Fig. 5). At 10 μg/mL TiO_2, nuclei (and eventually micronuclei) were covered by NPs, thus making the observation quite difficult.

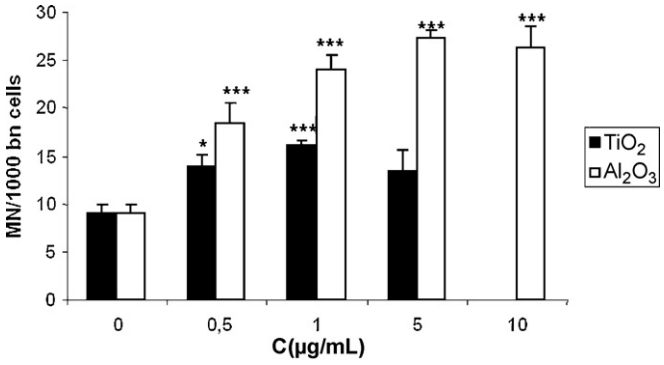

Fig. 5. Micronucleus induction in CHO-K1 cells after 24 h exposure to TiO_2 and Al_2O_3 nanoparticles. Significant difference at $^*p < 0.05$, $^{***}p < 0.001$. Data from the highest concentration (10 μg/mL) could not be measured due to cytotoxic effects.

3.5. TEM observations

TEM observations revealed that CHO-K1 cells treated with 50 μg/mL TiO_2 or Al_2O_3 NPs formed intracellular vesicles containing phagocyted material (Fig. 6). Fig. 6A–C shows TiO_2 agglomerates on both the surface and inside of CHO-K1 cells. Initial changes in the cell membrane previous to phagocytosis can be observed (Fig. 6C). Some of the particles were phagocyted by the cell and are included into a big vesicle. A portion of the plasma membrane is invaginated and pinched off to form a membrane-bound vesicle. Other NPs are free in different sites of the cell. It can be observed that all vesicles are present only in the cytoplasm and NPs could not enter into the nucleus. The nucleus shape is modified in the presence of some large vesicles which seem to press it. In some cells with many large vesicles, the membrane was disintegrated.

Al_2O_3 particle aggregates also induce the formation of vesicles within the cells. However, these aggregates are smaller than those formed in the presence of TiO_2 NPs (Fig. 6D and E).

4. Discussion

Nanotechnology development leads to the increasing use of nanomaterials. However, safety considerations such as the risk assessment of environment and human health have not paralleled industrial development, and consequently results are scarce [29]. In the present study, genotoxicity and cytotoxicity of TiO_2 and Al_2O_3 NPs were evaluated *in vitro* in CHO-K1 cells, which are particularly sensitive to NPs.

It is worth noting that cellular responses elicited by TiO_2 NPs are strongly dependent on NPs surface/mass ratio. Moreover, NPs toxicity also depends on chemical and structural characteristics (purity, crystallinity), surface properties (surface reactivity, adsorbed groups, coatings), solubility, shape, and aggregation [9]. In the same study, 20 nm anatase particles were found to be genotoxic while 200 nm did not induce toxicity [10,29]. Thus, the size, BET results, and TEM observations of the particles were included in the present work. Unfortunately, these details are not reported in several other studies and therefore the comparison of findings results quite difficult [10].

4.1. Evaluation of cytotoxic effects of TiO_2 and Al_2O_3 NPs

Several studies have shown cytotoxic effects of TiO_2 NPs on cancer cell lines as well as cultured human lymphoblastoid cells [30,31]. Our results show a loss of lysosomal activity by TiO_2 and Al_2O_3 NPs indicated by a decrease in NR uptake in CHO-K1 cells in a concentration-dependent manner. The way and quantity of responses are different: the effect of TiO_2 is stronger than that of Al_2O_3 NPs and begins at lower concentration. The NR assay showed a significant difference for 25 μg/mL TiO_2 and 100 μg/mL Al_2O_3 compared with control values. TiO_2 cytotoxicity was also determined by a significant reduction in lysosomal integrity in fish cells *in vitro* (RTG-2 cells) over 24 h exposure to 50 μg/mL [32]. Our previous results [33] with UMR106 showed that these cells are less sensitive to both Al_2O_3 and TiO_2; NR uptake for the NPs concentration range assayed in the present work did not show any decrease.

Alteration in the energetic cell metabolism induced by the NPs was further analyzed by the MTT assay measuring the ability of mitochondrial dehydrogenases. We found a significant decrease in MTT dye reduction in cells treated with NPs at low concentrations (5 μg/mL either TiO_2 or Al_2O_3). In agreement with our results, concentration-dependent cytotoxicity was observed in mouse fibroblasts (L929 cells) treated with TiO_2 NPs; slight changes were found at lower concentrations, and cell viability decreased drastically at higher concentrations (>6 μg/mL) [34]. Human cells seem to be less susceptible to NP toxicity than rodent cells; thus,

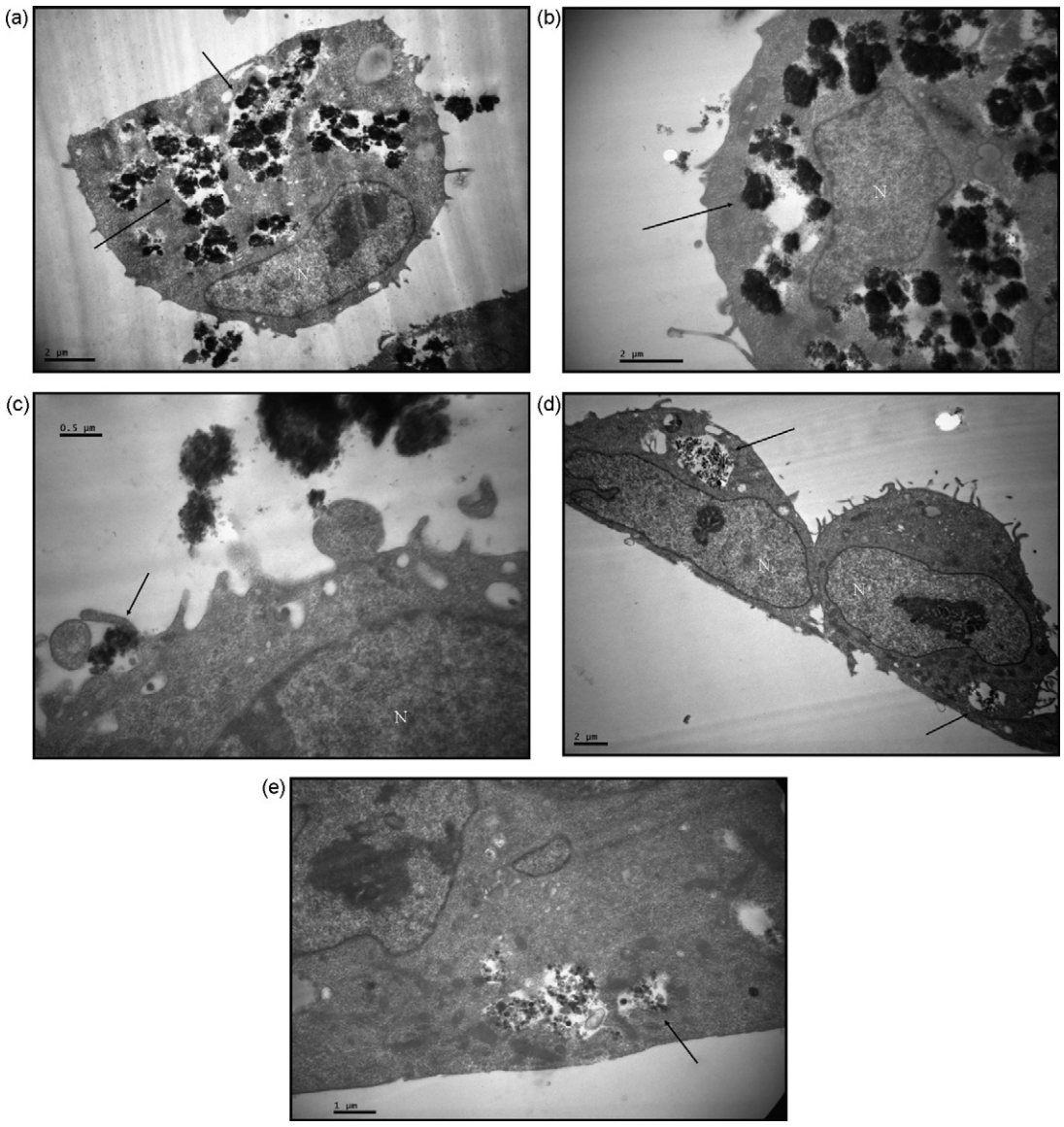

Fig. 6. TEM microphotographs from CHO-K1 cells exposed to 50 μg/mL TiO_2 (A, B, C) and 50 μg/mL Al_2O_3 (D, E) NPs for 24 h. Intracellular vesicles containing phagocyted material can be observed (black arrows). N: nucleus. (a) two of the largest vesicles seem to be coalescing (see arrow); (b) vesicles press the nucleus which is deformed (see arrow); (c) the beginning of an endocytosis process seems to be taking place (see arrow); (d) less compact aggregates of Al_2O_3 than those of TiO_2 can be observed (see arrow); (e) the limits of some vesicles are not well defined in some cases and seem to be disrupt.

no increased cytotoxicity could be observed in human bronchial epithelial cells exposed to 10 μg/cm^2 TiO_2 NPs [35] while significant cytotoxicity at lower concentrations (under our experimental conditions 5 μg/mL is equivalent to approximately 2 μg/cm^2) is reported in the present work. Furthermore, Hussain et al. [36] reported no measurable effect for TiO_2 at doses between 10 and 50 μg/mL but significant values at higher doses (100–250 μg/mL) in rat liver cells. Interestingly, our previous results from MTT assay with the same Al_2O_3 and TiO_2 NPs revealed a low but significant increase for 25, 50, and 100 μg/mL in UMR106 cells [33]. Consequently, NPs cytotoxic effect has shown to be concentration- and composition-dependent, and to differ from one cell line to another. Results from MTT assay evidenced toxicity before any effect with NR assay. They can be attributed to the eventual effect of NPs on mitochondria previous to any disruption on lysosomal activity, at least in CHO-K1 cell line. TiO_2 NPs have been suggested to disrupt mitochondrial function by the formation of reactive oxygen species (ROS) in several cell types such as brain microglia, bronchial epithelial cells, and peripheral lymphocytes [37–39].

Oxidative stress is defined as the disturbance in the prooxidant–antioxidants balance in favor of the prooxidant, leading to potential damage [40]. NPs can generate ROS through the interaction of the surface area with target cells. Moreover, oxidative stress produced by NPs inside the cell is well correlated with the BET surface area and NPs internalized amount [29]. Radicals produced under oxidative stress conditions induce a variety of lesions in DNA including strand breaks [41]. SCE induction has been also correlated with primary DNA damage [42]. The present report shows a low but significant increase in SCE frequencies only in those cells exposed to TiO_2 NPs; however Al_2O_3 NPs show no induction. This TiO_2 NPs SCE induction could be attributed to the wide surface area (three-fold higher than in Al_2O_3 NPs).

4.2. TEM observations

TEM observations revealed that NPs were present in the cell surroundings. These results agree with those from recent reports showing similar behavior for similar NPs. However, aggregates are

considered to be able to maintain the large surface/mass ratio and other characteristics of individual NPs [43].

Interestingly, TEM observations showed the formation of cellular vesicles in CHO-K1 cells after treatment with both NPs during 24 h. Shape of the cells and their nuclei seemed to be altered in presence of the vesicles. Cells turned more globular, their nuclei were pressed by the vesicles and their form was apparently modified. However, these effects could be the result of pre-treatments carried out to prepare samples for TEM observations. In accordance with flow cytometric analyses performed in mammalian cells with TiO_2 NPs [29], TEM microphotographs showed that the vesicles with individual particles and aggregates remained in the cytoplasm but not in the nucleus. This phenomenon was also observed for vascular endothelial cells treated with metal oxide NPs [44] and human pneumocytes [45]. Several types of NPs internalized into cells are often found within intracellular vesicles. Different mechanisms including phagocytosis, pinocytosis, or receptor-mediated endocytosis may induce the process of internalization also known as endocytosis. Ruan et al. [46] reported the formation of quantum dots-containing vesicles by macropinocytosis. This process is a fluid-phase endocytosis mechanism which occurs when NPs bind to negatively-charged cell membranes. Moreover, those particles that can enter the cells via the receptor-binding pathway would form circles of different size in the cytoplasm [47]. On the other hand, NPs uptake induced by simple pinocytosis could lead to the formation of clusters in the vesicle [48]. According to TEM micrographs, both types of NPs studied in this work formed NPs aggregation inside the vesicles and their internalization in lysosomal bodies arranged in perinuclear fashion, phenomenon that might be due to pinocytosis.

Consequently, the incorporation of NPs around the cells through endocytosis pathways during the first 24 h exposure could have disrupted lysosomal and mitochondrial activities. These events may probably induce a slowdown in the cell cycle (and thus in the proliferation rate index) and a decrease in cell viability.

We have previously reported a concentration-dependent inhibition of cell division in UMR106 cells treated with TiO_2 and Al_2O_3 NPs [33] although this cell cycle delay occurred after longer exposure periods. Our findings after TEM analysis also revealed the formation of cellular vesicles in UMR106 cells after treatment with both NPs during 24 h.

Commercially available NPs as those used in this work show different diameters with average values of 20 ± 7 and 28 ± 19 nm. Cellular response has been shown to depend on particles size. An interesting study by Gratton et al. [49] employed a top-down particle production technique to generate micro- and nano-hydrogel particles (with complete control of size, shape and surface) and Hela cells in their experiments. Their findings suggest that particles internalization is dependent on their size. Similarly, Chithrani and Chan [50] also reported that the mechanism of cellular uptake and removal of protein-coated gold nanoparticles depends on their size and shape as well as on the cell line used in the test. In this regard, our previous results showed a different response between UMR106 and CHO-K1 cells exposed to the same NPs. However, human cells seem to be less susceptible to particle toxicity than rodent cells.

4.3. Genotoxic effects of TiO_2 and Al_2O_3 NPs

Our results evidenced genotoxic effects on CHO-K1 cells exposed to TiO_2 and Al_2O_3 NPs. These findings are in agreement with previous studies demonstrating nanoparticle increased MN frequencies in cultured lymphoblastoid cells [31] and Syrian hamster embryo fibroblasts [51]. Moreover, significant induction of sister chromatid exchanges and MN was observed in CHO-K1 cells after exposure to TiO_2, even when not nanosized [19].

MN formation in CHO-K1 cells exposed to TiO_2 and Al_2O_3 NPs was also observed in the present study. Cells exposed to TiO_2-induced genetic damage at concentrations as low as 0.5 μg/mL in the MN assay. At higher concentration (>10 μg/mL), we could not find second-generation metaphases in the SCE assay. Additionally, the MN assay showed an inverted U-shape response revealing that a considerable number of cells had been affected by cytotoxic effects. In accordance, for the same concentration range, we found a relative increase in M1 cells and a fall in M2 cells (reduction of PRI, although not statistically different). Wang and co-workers [31] reported that cell division is inhibited after long exposure to TiO_2 NPs and that cytotoxicity may be due to transient inflammatory reactions. TiO_2-induced MN has been shown as the result of clastogenic events [51] since no significant increase in the kinetochore positive MN could be observed compared with unexposed control SHE fibroblast samples. The micronucleus can also be induced by chemicals that disrupt the mitotic spindle [52]. It has been suggested that the formation of MN may be due to physical disturbance of the particles around the mitotic apparatus [53]. Hence, the physical presence of large NPs aggregates might have affected the division process in these cells leading to chromosome loss rather than chromosome rupture. Findings on the lack of chromosome breakage were reported in CHO-WBL cells after treatment with different forms of rutile and anatase ultrafine TiO_2 particles, suggesting an aneugenic effect [16].

We shall now analyze our positive genotoxic results in the context of other reports. Bhattacharya et al. [35] demonstrated that TiO_2 NPs generated high levels of DNA adduct formation (detection of 8-hydroxyl-2-deoxyguanosine), probably due to the analysis of intra- and acellular ROS generation. Gurr et al. [54] have shown that TiO_2-NPs induce hydrogen peroxide and nitric oxide generation leading to lipid peroxidation and oxidative DNA damage in lung epithelial cells. Kang et al. [39] have observed the activation of DNA damage check-points and p53 up-regulation along with DNA damage caused by ROS generation by these nanoparticles in peripheral blood lymphocytes. Previous hypotheses could explain how the results here presented show that the particles induce genotoxicity if they do not enter the nucleus.

It is worth noting that Theogaraj et al. [16] did not find any increase in chromosomal aberration frequencies with TiO_2 NPs in CHO-K1 cell line in the presence or absence of UV radiation. However, exposure to NPs was too short (3 h). Similarly, Warheit et al. [17] did not show genotoxicity for this cell line after 4 h in activated condition using 65, 125, and 250 μg/mL TiO_2 NPs. Conversely, and in agreement with our results, Lu et al. [19] reported increased MN and SCE frequencies for 24 h exposure at concentrations as low as 5 μM (ca. 0.4 μg/mL). Zhu et al. [21] also observed a dose-dependent cytotoxic effect at 25–325 μg/mL concentration range for 24 h exposure. Consequently, former reports are not conflicting with the latter ones or results here presented, since 3 and 4 h exposure periods may not be long enough to detect genotoxic effects, indicating that the response is also dependent on the exposure time. Accordingly, general inference about NPs cytotoxicity and genotoxicity should not be solely based on assays of short exposure periods.

Our overall results showed the ability of two metal oxide NPs to induce both genotoxicity and cytotoxicity in vitro. Both NPs (Al_2O_3 and TiO_2) were found inside the cells forming vesicles, independently of their composition, but different sensitivity to each of them was observed. However, none of them entered the nucleus as in the case of gold particles of similar size [47]; this suggests that they express different modes on intracellular motility and enter mechanisms depending on the surface composition and size. We previously tested identical NPs with UMR106 cells with dissimilar results [33] revealing that the toxic response is strongly dependent on the cell line employed. Comparison with other reports showed

that cytotoxic and genotoxic responses in CHO-K1 cells also depend on the exposure period. Further studies are required in order to analyze the mechanisms behind the effects observed.

Acknowledgements

This study was supported by: Agencia Nacional de Promoción Científica y Tecnológica (grant BID 1728 OC/AR PICT 0533225; PICT 05-32906; PAE 22771), Universidad Nacional de La Plata (grant 11-05I-129), and Consejo Nacional de Investigaciones Científicas y Técnicas (PIP 6075). Dr. Arnal thanks Prof. F.Schüth at Max Planck Institut für Kohlenforschung for supporting nanoparticles characterization by TEM and Nitrogen Sorption.

References

[1] M.N. Rittner, Market analysis of nanostructured materials, Am. Ceram. Soc. Bull. 81 (2002) 33–36.
[2] G. Oberdoerster, E. Oberdoerster, J. Oberdoerster, Nanotoxicology: an emerging discipline evolving from studies of ultrafine particles, Environ. Health Perspect. 113 (7) (2005) 823–839.
[3] R. Paull, J. Wolfe, P. Hebert, M. Sinkula, Investing in nanotechnology, Nat. Biotechnol. 21 (10) (2003) 1144–1147.
[4] V.L. Colvin, The potential environmental impact of engineered nanomaterials, Nat. Biotechnol. 21 (2003) 1166–1170.
[5] K. Donaldson, D. Brown, A. Clouter, R. Duffin, W. MacNee, L. Renwick, L. Tran, V. Stone, The pulmonary toxicology of ultrafine particles, J. Aerosol. Med. 15 (2002) 213–220.
[6] V. Stone, J. Shaw, D.M. Brown, W. MacNee, S.P. Faux, K. Donaldson, The role of oxidative stress in the prolonged inhibitory effect of ultrafine carbon black on epithelial cell function, Toxicol. In Vitro 12 (1998) 649–659.
[7] G. Oberdörster, J.N. Finkelstein, C. Johnston, R. Gelein, C. Cox, R. Baggs, A.C. Elder, Acute pulmonary effects of ultrafine particles in rats and mice, Res. Rep. Health Eff. Inst. 96 (2000) 5–74.
[8] T.J. Brunner, P. Wick, P. Manser, P. Spohn, R. Grass, L.K. Limbach, A. Bruinink, W.J. Stark, In vitro cytotoxicity of oxide nanoparticles: comparison to asbestos, silica, and the effect of particle solubility, Environ. Sci. Technol. 40 (2006) 4374–4381.
[9] A. Nel, T. Xia, L. Madler, N. Li, Toxic potential of materials at the nanolevel, Science 311 (2006) 622–627.
[10] N. Singh, B. Manshian, G.J. Jenkins, S.M. Griffiths, P.M. Williams, T.G. Maffeis, C.J. Wright, Nanogenotoxicology: the DNA damaging potential of engineered nanomaterials, Biomaterials 30 (2009) 3891–3914.
[11] A. Banasik, A. Lankoff, A. Piskulak, K. Adamowska, H. Lisowska, A. Wojcik, Aluminum-induced micronuclei and apoptosis in human peripheral-blood lymphocytes treated during different phases of the cell cycle, Environ. Toxicol. 20 (2005) 402–406.
[12] A. Lankoff, A. Banasik, A. Duma, E. Ochniak, H. Lisowska, T. Kuszewski, S. Góźdź, A. Wojcik, A comet assay study reveals that aluminium induces DNA damage and inhibits the repair of radiation-induced lesions in human peripheral blood lymphocytes, Toxicol. Lett. 161 (2006) 27–36.
[13] P.D.L. Lima, D.S. Leite, M.C. Vasconcellos, B.C. Cavalcanti, R.A. Santos, L.V. Costa-Lotufo, C. Pessoa, M.O. Moraes, R.R. Burbano, Genotoxic effect of aluminium chloride in cultured human lymphocytes treated in different phases of cells cycle, Food Chem. Toxicol. 45 (2007) 1154–1159.
[14] A. Balasubramanyam, N. Sailaja, M. Mahboob, M.F. Rahman, S. Misra, S.M. Hussain, P. Grover, Evaluation of genotoxic effects of oral exposure to aluminum oxide nanomaterials in rat bone marrow, Mutat. Res. 676 (2009) 41–47.
[15] A.J. Wagner, C.A. Bleckmann, R.C. Murdock, A.M. Schrand, J.J. Schlager, S.M. Hussain, Cellular interaction of different forms of aluminum nanoparticles in rat alveolar macrophages, J. Phys. Chem. B 111 (2007) 7353–7359.
[16] E. Theogaraj, S. Riley, L. Hughes, M. Maier, D. Kirkland, An investigation of the photo-clastogenic potential of ultrafine titanium dioxide particles, Mutat. Res. 634 (2007) 205–219.
[17] D.B. Warheit, R.A. Hoke, C. Finlay, M. Donner, K.L. Reed, C.M. Sayes, Development of a base set of toxicity tests using ultrafine TiO_2 particles as a component of nanoparticle risk management, Toxicol. Lett. 171 (2007) 99–110.
[18] Y. Nakagawa, S. Wakuri, K. Sakamoto, N. Tanaka, The photogenotoxicity of titanium dioxide particles, Mutat. Res. 394 (1997) 125–132.
[19] P.J. Lu, I.C. Ho, T.C. Lee, Induction of sister chromatid exchanges and micronuclei by titanium dioxide in Chinese hamster ovary—K1 cells, Mutat. Res. 414 (1998) 15–20.
[20] T. Uchino, H. Tokunaga, M. Ando, H. Utsumi, Quantitative determination of OH radical generation and its cytotoxicity induced by TiO(2)-UVA treatment, Toxicol. In Vitro 16 (2002) 629–635.
[21] R.R. Zhu, S.L. Wang, J. Chao, D. Lu Shi, R. Zhang, X.Y. Sun, S.D. Yao, Bio-effects of nano-TiO2 on DNA and cellular ultrastructure with different polymorph and size, Mater. Sci. Eng. C 29 (2009) 691–696.
[22] G. Fotakis, J.A. Timbrell, In vitro cytotoxicity assys: comparison of LDH, neutral red, MTT and protein assay in protein assay in hepatoma cell lines following exposure to cadmium chloride, Toxicol. Lett. 160 (2006) 171–177.
[23] T.F. Slater, B. Sawyer, U.D. Strauli, Studies on succinate–tetrazolium reductase systems. III. Points of coupling of four different tetrazolium salts, Biochim. Biophys. Acta 77 (1963) 383–393.
[24] E. Borenfreund, J.A. Puerner, A simple quantitative procedure using monolayer culture for toxicity assays, J. Tissue Cult. Methods 9 (1984) 7–9.
[25] T. Mosmann, Rapid colorimetric assay for cellular growth and survival: application to proliferation and cytotoxicity assays, J. Immunol. Methods 65 (1983) 55–63.
[26] S.P. Wolff, P. Perry, New Giemsa method for differential staining of sister chromatids, Nature 261 (1974) 156–158.
[27] L. Lamberti, P. Bigatti-Ponzetto, G. Ardito, Cell kinetics and sister chromatid exchange frequency in human lymphocytes, Mutat. Res. 120 (1983) 193–199.
[28] M. Fenech, The in vitro micronucleus technique, Mutat. Res. 455 (2000) 81–95.
[29] H. Suzuki, T. Toyooka, Y. Ibuki, Simple and easy method to evaluate uptake potential of nanoparticles in mammalian cells using a flow cytometric light scatter analysis, Environ. Sci. Technol. 41 (2007) 3018–3024.
[30] P. Thevenot, J. Cho, D. Wavhal, R.B. Timmons, L. Tang, Surface chemistry influences cancer killing effects of TiO_2 nanoparticles, Nanomedicine 4 (2008) 226–236.
[31] J.J. Wang, B.J.S. Sanderson, H. Wang, Cyto- and genotoxicity of ultrafine TiO_2 particles in culture human lymphoblastoid cells, Mutat. Res. 628 (2007) 99–106.
[32] W.F. Vevers, A.N. Jha, Genotoxic and cytotoxic potential of titanium dioxide (TiO_2) nanoparticles on fish cells in vitro, Ecotoxicology 17 (2008) 410–420.
[33] A.L. Di Virgilio, M. Reigosa, M. Fernández Lorenzo, Response of UMR 106 cells exposed to titanium oxide and aluminium oxide nanoparticles, J. Biomed. Mater. Res. 92A (2010) 80–86.
[34] C.Y. Jin, B.S. Zhu, X.F. Wang, Q.H. Lu, Cytotoxicity of titanium dioxide nanoparticles in mouse fibroblast cells, Chem. Res. Toxicol. 21 (2008) 1871–1877.
[35] K. Bhattacharya, M. Davoren, J. Boertz, R.P.F. Schins, E. Hoffmann, E. Dopp, Titanium dioxide nanoparticles induce oxidative stress and DNA-adduct formation but not DNA-breakage in human lung cells, Parti. Fibre Toxicol. 6 (2009) 17–27.
[36] S.M. Hussain, K.L. Hess, J.M. Gearhart, K.T. Geiss, J.J. Schlager, In vitro toxicity of nanoparticles in BRL 3A rat liver cells, Toxicol. In Vitro 19 (2005) 975–983.
[37] T.C. Long, J. Tajuba, P. Sama, N. Saleh, C. Swartz, J. Parker, S. Hester, G.V. Lowry, B. Veronesi, Nanosized titanium dioxide stimulates reactive oxygen species in brain microglia and damages neurons in vitro, Environ. Health Perspect. 115 (2007) 1631–1637.
[38] E.J. Park, J. Yi, K.H. Chung, D.Y. Ryu, J. Choi, K. Park, Oxidative stress and apoptosis induced by titanium dioxide nanoparticles in culture BEAS-2B cells, Toxicol. Lett. 180 (2008) 222–229.
[39] S.J. Kang, B.M. Kim, Y.J. Lee, H.W. Chung, Titanium dioxide nanoparticles trigger p53-mediated damage response in peripheral blood lymphocytes, Environ. Mol. Mutagen. 49 (2008) 399–405.
[40] H. Sies, What is oxidative stress? in: J.F. Keaney Jr. (Ed.), Oxidative Stress and Vascular Disease, Kluwer Academic Publishers, Boston, 2000, pp. 1–8.
[41] M.K. Shigenaga, B.N. Ames, Assays for 8-hydroxy-2′-deoxyguanosine a biomarker of in vivo oxidative DNA damage Free Radic. Biol. Med. 10 (1991) 211–216.
[42] E.M. Parry, J.M. Parry, In vitro cytogenetics and aneuploidy, in: D.H. Philipps, S. Venitt (Eds.), Environmental Mutagenesis, BIOS Scientific Publishers Limited, Oxford, 1995, pp. 121–135.
[43] S. Hussain, S. Boland, A. Baeza-Squiban, R. Hamel, L.C.J. Thomassen, J.A. Martens, M.A. Billon-Galland, J. Fleury-Feith, F. Moisan, J.C. Pairon, F. Marano, Oxidative stress and proinflammatory effects of carbon black and titanium dioxide nanoparticles: role of particle surface area and internalized amount, Toxicology 260 (2009) 142–149.
[44] A. Gojova, B. Guo, R.S. Kota, J.C. Rutledge, I.M. Kennedy, A.I. Barakat, Induction of inflammation in vascular endothelial cells by metal oxide nanoparticles: effect of particle composition, Environ. Health Perspect. 115 (2007) 403–409.
[45] A. Simon-Deckers, B. Gouget, M. Mayne-L'hermite, N. Herlin-Boime, C. Reynaud, M. Carrière, In vitro investigation of oxide nanoparticle and carbon nanotube toxicity and intracellular accumulation in A549 human pneumocytes, Toxicology 253 (2008) 137–146.
[46] G. Ruan, A. Agrawal, A.I. Marcus, S. Nie, Imaging and tracking of Tat peptide-conjugated quantum dots in living cells: new insights into nanoparticle uptake, intracellular transport, and vesicle shedding, J. Am. Chem. Soc. 129 (2007) 14759–14766.
[47] H.J. Yen, S.H. Hsu, C.L. Tsai, Cytotoxicity and Immunological Response of Gold and Silver Nanoparticles of Different Sizes, Small 5 (2009) 1553–1561.
[48] R. Shukla, V. Bansal, M. Chaudhary, A. Basu, R.R. Bhonde, M. Sastry, Biocompatibility of gold nanoparticles and their endocytotic fate inside the cellular compartment: a microscopic overview, Langmuir 21 (2005) 10644–10654.
[49] S.E. Gratton, P.A. Ropp, P.D. Pohlhaus, J.C. Luft, V.J. Madden, M.E. Napier, J.M. DeSimone, The effect of particle design on cellular internalization pathways, Proc. Natl. Acad. Sci. U.S.A. 105 (2008) 11613–11618.
[50] B.D. Chithrani, W.C. Chan, Elucidating the mechanism of cellular uptake and removal of protein-coated gold nanoparticles of different sizes and shapes, Nano Lett. 7 (2007) 1542–1550.
[51] Q. Rahman, M. Lohani, E. Dopp, H. Pemsel, L. Jonas, D.G. Weiss, D. Schiffmann, Evidence that ultrafine titanium dioxide induces micronuclei and apoptosis in Syriam hamster embryo fibroblast, Environ. Health Perspect. 220 (2002) 797–800.

[52] J.M. Parry, An evaluation of the use of in vitro tubulin polymerization, fungal and wheat assays to detect the activity of potential chemical aneugens, Mutat. Res. 287 (1993) 23–28.
[53] T.W. Hesterberg, C.J. Butterick, M. Oshimura, A.R. Brody, J.C. Barrett, Role of phagocytosis in Syrian Hamster cell transformation and cytogenetic effects induced by asbestos and short and long glass fibers, Cancer Res. 46 (1986) 5795–5802.
[54] J.R. Gurr, A.S. Wang, C.H. Chen, K.Y. Jan, Ultrafine titanium dioxide particles in the absence of photoactivation can induce oxidative damage to human bronchial epithelial cells, Toxicology 213 (2005) 66–73.